International Journal of Rotating Machinery, 9(3): 163–170, 2003

1023-621X/03 $12.00 + .00
DOI: 10.1080/10236210390147308

Taylor & Francis
Taylor & Francis Group

Cavitating Flow Calculations in Industry

Philippe Dupont
Sulzer Pumps, Ltd., Winterthur, Switzerland

Tomoyoshi Okamura
Hitachi Industries Co., Ltd., Ibaraki, Japan

This paper presents the experiences of two pump manufacturers with numerical cavitation prediction methods available in commercial computational fluid dynamic software or in codes developed in-house. The intention of the authors is to evaluate these methods and their capabilities in predicting the cavitating performance of pumps from an industrial point of view.

In the first part of the article, benchmarks were set for three different commercial software packages on the basis of a comparison of measurements obtained for a centrifugal pump. In the second part, the results of a commercial code are compared, for different impellers, to those obtained with a simplified cavitation prediction code.

The abilities and the benefits of the various approaches to cavitation prediction in the design process of a pump are discussed.

Keywords Cavitation, CFD, Pumps

The usage of numerical tools to design and optimize the hydraulics of pumps is nowadays a standard in the industry (Casartelli, 1995; Goto, 1997; Zangeneh et al., 1996, 1998). Until now, this optimization has focused mainly on the efficiency and stability of the head curve through better control of the recirculation and through reduction of secondary flows. As a matter of fact, the cavitation is also a major limiting factor in pump design. Nevertheless, only few attempts to improve cavitation in pumps by using numerical approaches have been made. Most of the time, this optimization is limited to finer adaptation of vane inlet angles based on the predicted flow angles obtained from analysis of cavitation free flow computational fluid dynamics (CFD) and to improvement of the profiling of the vanes in order to limit the minimum pressure (Śpring, 1992).

In recent decades, models for the prediction of cavitation have been refined and successfully applied on isolated two-dimensional profiles for steady flows (Dupont and Avellan, 1991; Favre et al., 1987; Lemonnier and Rowe, 1988; Uhlman, 1983; Ukon, 1980) and for unsteady flows (Delannoy, 1989; Delannoy and Kueny, 1990; Kubota et al., 1989, 1992). In the same period, a few three-dimensional models based on potential (Kinnas and Fine, 1993), on S1/S2, or on Euler (Kaenel et al., 1995; Maitre et al., 1990) have been developed and applied, but no one is taking into account the three-dimensional turbulent and viscous effects of the cavity on the mean flow.

More recently, some of these methods have been introduced in three-dimensional Reynolds-averaged Navier-Stokes codes. The various approaches can be differentiated:

- A single-fluid model with empirical state law that defines the density variation of a liquid-vapor mixture (Reboud et al., 1998);
- A volume-of-fluid method based on a two-phase approach where the convection of one phase in a second phase is calculated, with a possible mass exchange between the two phases based on a law of the state (Dieval et al., 1998);
- A cavity-interface tracking method, which iteratively adapts the cavity shape in order to reach a given condition (velocity or pressure) at its interface (Hirschi et al., 1998a);

Received 28 March 2002; accepted 28 March 2002.

The authors thank the managements of Hitachi Industries Co., Ltd., Ibaraki, Japan, and Sulzer Pumps, Ltd., Winterthur, Switzerland, for permission to publish this paper. The tests presented in the first part of the article were made possible thanks to the support of the Cavitation Research Committee of the Turbo-machinery Society of Japan. CFD calculations presented in this part of the article were performed, for CFX-Tascflow, by AEA Hyprotech KK; for STAR-CD, by CD-adapco Japan Co., Ltd.; and for Fluent, by Fluent Asia Pacific, Ltd. The CFX-Tascflow calculations presented in the second part of the article were performed by Sulzer Innotec. The authors also extend their thanks to Professor Tsujimoto who initiated the idea of this joint paper about the industrial experience of two different pump manufacturers.

Address correspondence to Dr. Philippe Dupont, Sulzer Pumps, Ltd., Zurcherstrasse 12, Winterthur, 8401, Switzerland. E-mail: philippe.dupont@sulzer.com

- A bubbly two-phase flow model solving a Rayleigh-Plesset equation in order to calculate the density of a mixture of water and bubbles (Tamura et al., 2001).

Most of the commercial CFD packages commonly used in the fluid machinery industry have introduced one of these cavitation prediction models. However, these methods have been only recently introduced in these codes and, therefore, there is a very small return of experience in the usage of such methods, especially in an industrial context (Combes and Archer, 2000; Visser, 2001). It is the purpose of this article to provide some information about the ability of these methods to predict cavitation in pumps and, in a provocative way, to compare their results to a simplified prediction method based on the postprocessing of a noncavitating flow calculation, corresponding to a noncoupled approach, supposing that the cavitation development does not affect the liquid flow.

BENCHMARK OF COMMERCIAL CODES

Tested Pump

The tested pump is shown in Figure 1. Professors R. Oba and H. Soyama of Tohoku University carried out the experiments in 1993 (Soyama, 1995). The main purpose of the test was to obtain precise data on cavitation erosion of the impeller. The research committee concerning the cavitation damage of pumps in the Turbomachinery Society of Japan supported the study of this pump. The impeller is designed so as to simulate the inlet flow in the boiler feed pump. For this reason, the impeller has a high hub ratio. The design rotational speed is 6350 min^{-1}, but the cavitation appearances were observed at 3000 min^{-1}. The precise measured data of cavitation, such as incipient point, cavity length, and thickness, were not obtained.

Computation

Three commercial codes—CFX-Tascflow, FLUENT, and STAR-CD—were examined for this benchmark test. Each software vender was responsible for the mesh generation and computation. The methods used for the cavitation calculation in the various codes are not described in this article. The reader is asked to refer to the manuals of these codes for more information.

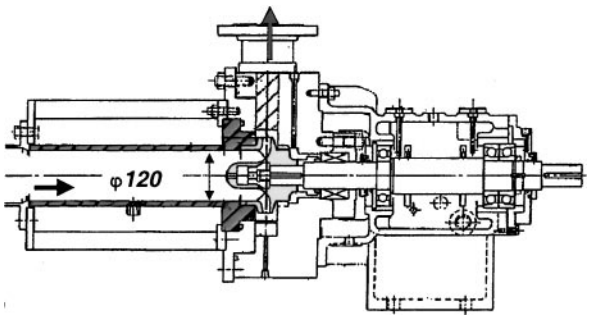

FIGURE 1
The double-volute centrifugal pump that was tested.

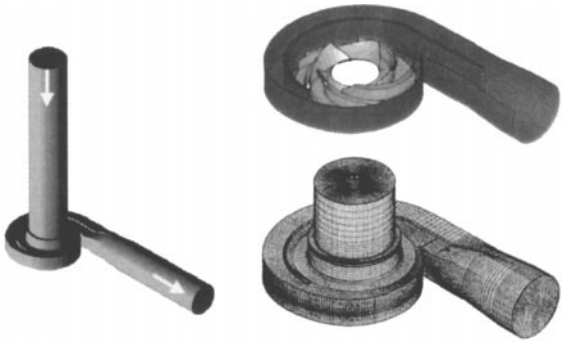

FIGURE 2
Computational mesh used for STAR-CD (400,000 unstructured elements).

CFX-Tascflow (Ver. 2.10)

One flow passage of the pump impeller was analyzed, so the computing time was short, about 30–50 min per case. Grid size was as follows: in-block part, $12 \times 39 \times 25$; main part, $57 \times 39 \times 25$; and out-block part, $13 \times 39 \times 25$. A frozen/rotor sliding interface was applied. Twenty-nine different inlet pressure levels were calculated at the best efficiency flow rate. The calculations were also made at 80% and 120% of the best efficiency flow rate.

FLUENT

The unsteady flow in the whole pump passage was analyzed. It took about 1 day per case to obtain the result. Therefore, only the best efficiency flow rate was analyzed.

STAR-CD

The unsteady flow in the whole pump passage (400,000 meshes) was analyzed. This computation was made almost 3 years ago, and at that time it took about 1 month for five cases. Noncavitating flow analysis was also made and compared with the results at high net positive suction head (NPSH). As for FLUENT, only the best efficiency flow rate was calculated.

Computational Results

CFX-Tascflow (Ver. 2.10)

The calculated cavitation performance is shown in Figure 3. The computational results do not include the head losses, except for the impeller flow passage. For this reason, the calculated total head shows a higher value than the experimental one. A reasonable computing time allows 29 different suction pressure levels to be analyzed. The phenomenon of head impairment can be clearly seen. The predicted NPSH where the 3% drop in total head occurs agrees fairly well with the experimental one. The predicted cavitation length is observed to be a little bit longer than the experimental one.

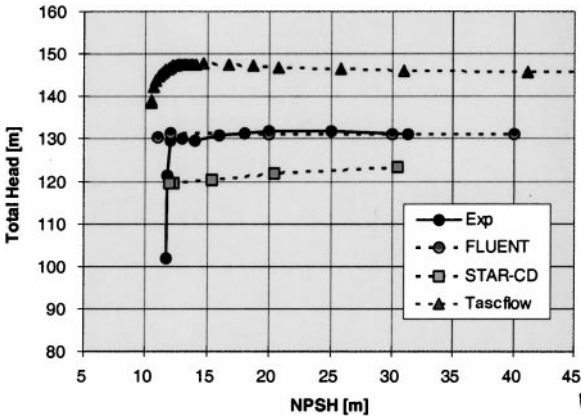

FIGURE 3
Head drop predicted by the codes (FLUENT, STAR-CD, and CFX-Tascflow), as compared to measurements.

FLUENT

The predicted cavitation performance is also given in Figure 3. A good agreement of total head is observed between calculation and experiment at the highest pressure levels. As the calculation time is important, only 5 points are calculated. The head impairment can therefore not be seen clearly. Nevertheless, the total head at the lowest NPSH is lower by about 1% than that it is in a noncavitating condition. The cavity patterns for NSPH equal to 30, 20, and 12 m are shown in Figure 4.

STAR-CD

The cavitation performance calculated by STAR-CD was compared with the measured one (Fig. 6). The agreement between the calculated and the experimental head is not so good. Coarse meshes and an inadequate turbulence model may be the reasons for these discrepancies, but the predicting accuracy of the head drop NPSH is reasonable. The predicted cavitation appearances are shown in Figure 5. The cavity thickness is also given in this figure; the cavity thickness at the vane inlet seems to have been overestimated.

Comparison

The comparison of the cavitation development predicted by the three different codes is given in Figure 6. Thanks to the number of suction pressure levels analyzed, CFX-Tascflow gives a much better head drop prediction then do the two other codes. Because of the modelization of the whole pump, the prediction of a noncavitating head by FLUENT agrees well with the measurement. However, the predicted head impairment due to cavitation is significantly underestimated by this code.

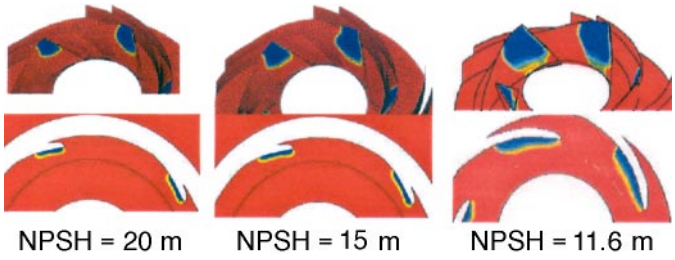

FIGURE 5
Cavity pattern for NPSH = 20, 15, and 11.6 m predicted by STAR-CD.

NONCOUPLED VERSUS COUPLED APPROACH

In the development of a surface tracking method for the prediction of attached cavitation (Hirschi, 1997, 1998a, 1998b), an initial cavity shape corresponding to the envelope of a bubble in evolution over a blade has been used. The comparison of the results obtained with this approach and the experimental data has shown the initial cavity shape to be very close to the measured one for moderate cavity length. This has been observed to be true as long as cavity development does not affect the main flow and the cavity does not reach the throat of the blade-to-blade channel. It has been proposed to use the initial cavity shape developed in the original method without applying the surface tracking method, in order to have a fast estimation of the cavity length. Dupont (2001) has described this method in detail. Only the basics of the method are given here. This corresponds to a decoupled approach, compared to the above-mentioned methods, as the effects of the cavity development on the liquid flow are not taken into account.

The results of this simplified method were then compared to those obtained with the cavitation model of CFX-Tascflow.

FIGURE 4
Cavity pattern for NPSH = 30, 20, and 12 m, as predicted by FLUENT.

FIGURE 6
Comparison of cavity prediction by the various codes.

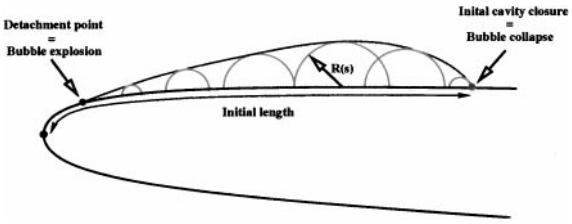

FIGURE 7
Bubble envelope taken as the initial cavity shape.

Description of the Noncoupled Cavitation Prediction Code

The cavity shape is calculated by solving a normalized form of the well-known Rayleigh–Plesset equation. It is supposed that the envelope of bubbles in evolution over the profile can approach the cavity shape, as shown in Figure 7.

The radius, instead of the diameter, of the bubble is chosen to define this envelope. This is based on the experimental observation of a hemispherical shape of the bubbles in evolution along a solid wall and on a measured height of these bubbles, corresponding roughly to their radius (Arn et al., 1998).

For each operating point and inlet pressure level that is analyzed, the Rayleigh–Plesset equation is solved on five streamlines, from hub to shroud, along the suction and the pressure sides of an impeller vane, using the pressure distribution obtained by a three-dimensional Navier–Stokes calculation for the noncavitating condition.

A typical nucleus size is chosen to initiate the calculation. A comparison is made of the nucleus size with the critical radius according to the minimum pressure over the impeller vane. If the critical size is too small to ensure the explosive development of the nuclei, the calculation is not performed and the operating point is considered free of cavitation or corresponding to development of isolated bubbles.

Cavity Length

The calculation of bubble growth and collapse gives a rapid estimation of the detachment and the closure locations of the attached cavity, as shown in Figure 7. The cavity length is then defined as the collapse location of the bubbles. An example of the predicted cavity length, divided by the impeller mean outlet radius, is given in Figure 8 as a function of the cavitation coefficient value. The nonhomogeneous cavity development along the span of the vane is very well illustrated in this example. The cavity develops much sooner at the shroud than at the hub, as expected because of the higher relative velocity on the external streamline.

The incipient cavitation coefficient is defined as the first nonzero cavity length along the vane span, as shown for the example given in Figure 8. Because of surface tension and bubble dynamic effects, this value does not correspond to the minimum pressure coefficient along the vane. For this reason, the prediction of the incipient cavitation coefficient based only on the minimum pressure calculated from the cavitation free condition is wrong.

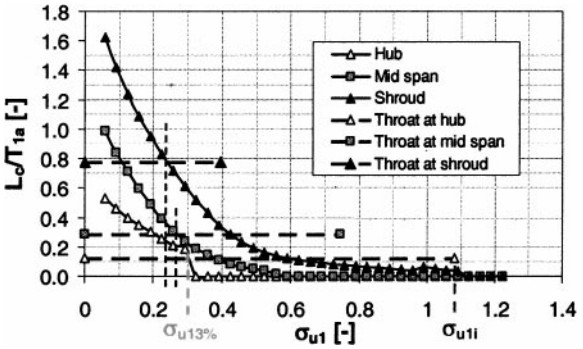

FIGURE 8
Predicted (Neptune) cavity length as a function of the sigma value along three streamlines.

As this incipient condition is quite difficult to determine on the test bed and depends on the quality of the water, a cavity length of 1% of the impeller mean outlet diameter is used in practice as a criterion for the cavitation inception. It is this criterion that will be compared to the measurement in the application examples presented hereafter.

Performance Impairment

With the fully coupled methods, the performance impairment can be directly calculated based on the modification of the flow due to the cavity's development. In this simplified approach, the prediction of the beginning of the performance impairment due to cavitation is made on the basis of the cavity length and the cavity thickness. The impairment is supposed to take place when the cavity induces a blockage in the flow. When the cavity reaches the blade-to-blade channel throat, along the suction and/or the pressure side of the blade, the section area of the cavity is compared to the throat area. When the ratio of these areas reached a certain threshold, the $\sigma_{3\%}$ condition is supposed to have been reached. This threshold has been experimentally determined.

The comparison with experimental results made in this article shows the method to give quite accurate results as far as the throat of the blade-to-blade channel is correctly calculated.

These blade-to-blade throat positions are given along the different streamlines by the horizontal dotted lines in Figure 8; a $\sigma_{3\%}$ of 0.3 is predicted. It has to be noted that the head impairment is caused by the cavity's reaching the blade-to-blade throat at the hub even if the cavity starts to develop at the shroud much sooner than at the hub. This occurs because the throat area is positioned more downstream at shroud than at the hub, allowing a larger cavity to develop before reaching the blade-to-blade throat. It shows the necessity of calculating accurately the cavity length as a function of the cavitation coefficient so as to be able to predict the associated head impairment.

A possible physical explanation of the correlation between the beginning of the head impairment and the cavity entering

the blade-to-blade throat is the influence of the wake of the cavity on the velocity field at the impeller outlet. As shown by Hirschi (1998a) from Navier–Stokes calculations including the attached cavity, the wake of the cavity is drastically reduced when reaching the blade-to-blade throat due to the relative flow acceleration. No modification of the velocity profiles at the impeller outlet is then observed. On the contrary, when the cavity is inducing a blockage in the throat area, there is no more reduction of the wake, resulting in a significant change in the velocity distribution at the impeller outlet that can lead to the head drop. It can also be a possible explanation of the difference observed between calculated and measured head impairment when calculating the cavitating flow in the impeller only. As the cavity development is modifying the impeller outlet flow, one can imagine this modification to have an influence on the efficiency of the diffuser as well.

Comparison Between CFX-Tascflow and Neptune

In order to assess the ability of the coupled (CFX-Tascflow) and decoupled (Neptune) approaches to predict effects of small geometrical changes on cavitation development, measurements were compared to the predicted cavitation development. These measurements were obtained for two different impellers of the same diffuser pump of a specific speed of nq = 33 (1700 in U.S. units). The differences between the two impellers are a small modification of the blade inlet angles, a change in the blade development close to the leading edge, and a modification in the shroud's meridional contour (Fig. 9). These modifications were introduced in order to improve the cavitation inception characteristics of the original impeller. These two impellers were machined using computer numerical control so as to obtain the most relevant comparison.

For this comparison, and contrary to the previously presented results, it was not the code vendor but Sulzer Innotec, the research center of Sulzer, that performed the CFX-Tascflow calculations. As for the previous results, only the impeller was taken into account in the calculation. The mesh used for this second study was created using a proprietary automatic elliptic grid generator. About 150,000 nodes were used to mesh a blade-to-blade channel of the impeller. The usage of this commercial code for performance prediction of pumps of different specific speed has been intensively validated (Guelich, 1997; Muggli et al., 1997).

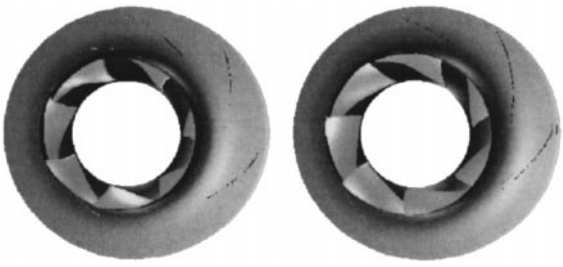

FIGURE 9
Original (left) and modified (right) impellers.

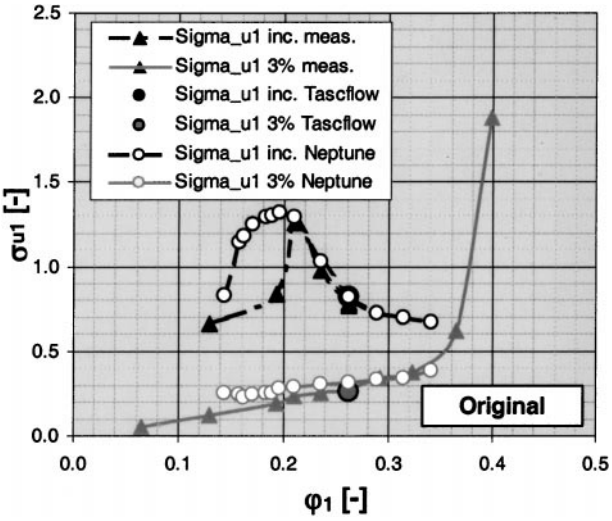

FIGURE 10
Measured and predicted (CFX-Tascflow and Neptune) inception and 3% head impairment curves in the original impeller.

Original Impeller

The measurements of the original impeller were compared to the prediction of the two codes in Figure 10. The inception and 3% head drop results are used for this comparison. The cavitation prediction using the noncoupled code (Neptune) was performed for 13 operating points from 50% to 130% of the BEP. The total time needed for this cavitation analysis was about 2 hr on a standard workstation. About 80 suction pressure levels, from cavitation inception to full cavitation, were used to calculate the cavity length evolution for each operating point. Together with the Navier-Stokes calculation (CFX-Tascflow) previously done for each flow condition, so as to obtain the noncavitating pressure distribution over the blade, the total analysis time for an impeller was about 1 day.

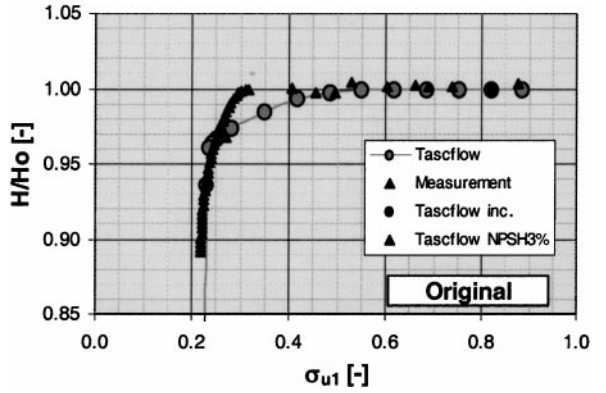

FIGURE 11
Measured and predicted (CFX-Tascflow) relative head impairment as a function of the cavitation index of the original impeller.

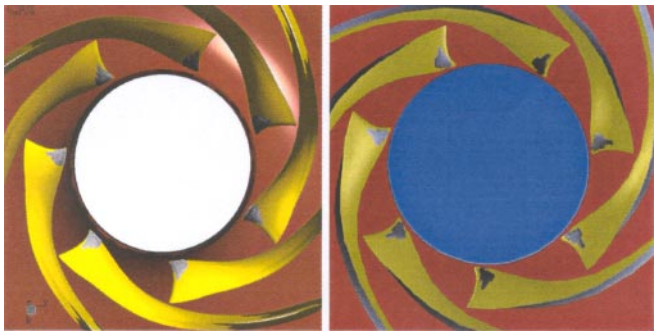

FIGURE 12
Predicted cavity for $\sigma_{u1} = 0.8$ for the original impeller at the best efficiency point ($\varphi_1 = 0.26$) (left: CFX-Tascflow; right: Neptune).

The cavitation analysis using the cavitation module of CFX-Tascflow was done only for the BEP. The calculation was done in the impeller alone. The inlet pressure level was gradually decreased in 13 steps from the noncavitating to the full cavitating condition. The time needed for this calculation was about 50 hr. The variation between the calculated head and the noncavitating head is compared to the measured one in Figure 11.

As shown by the comparison with the measurements given in Figure 10, the two methods predict very well the inception and 3% head impairment limits for the BEP. The front views of the impeller with cavity development given in Figures 12 and 13 for a σ_{u1} of 0.8 and 0.3, respectively, show good concordance between the two methods, even if the cavities predicted by CFX-Tascflow are slightly shorter and significantly thicker.

The evolution of the head impairment with the cavitation coefficient calculated by CFX-Tascflow was compared to the measurement (Fig. 11). One can observe in this figure that, even if the 3% head impairment as well as the full cavitation limits are very well, the calculation shows an earlier impairment than that which was measured.

The results obtained with Neptune for the other operating points show a fairly good agreement with the measured one.

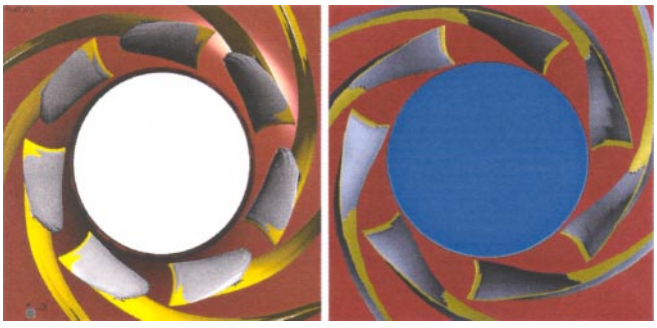

FIGURE 13
Predicted cavity for $\sigma_{u1} = 0.3$ for the original impeller at the best efficiency point $\varphi_1 = 0.26$) (left: CFX-Tascflow; right: Neptune).

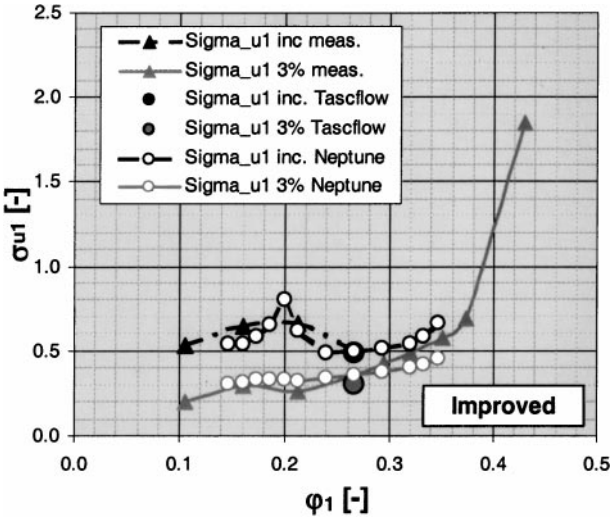

FIGURE 14
Measured and predicted (CFX-Tascflow and Neptune) inception and 3% head impairment curves for the improved impeller.

Even the drop of the cavitation inception at part load due to the development of impeller inlet recirculation is underestimated. This discrepancy could be due the effect of the diffuser on the recirculation pattern, not taken into account in this calculation.

Improved Impeller

A new improved impeller has been designed in order to reduce the cavitation inception at partload. A comparison of the results obtained from the two measurement approaches was also made for the improved impeller at the BEP. As for the original impeller, the predicted inception and 3% head impairment compared well with measurements, as shown in Figure 14. In particular, the measured improvement of cavitation inception was very well reproduced by the two different methods.

The cavity development as calculated by the two methods is presented in Figures 15 and 16 for the cavitation coefficients

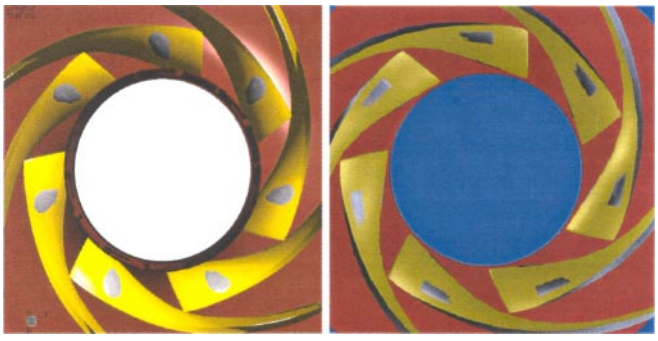

FIGURE 15
Predicted cavity for $\sigma_{u1} = 0.5$ for the improved impeller at the best efficiency point ($\varphi_1 = 0.26$) (left: CFX-Tascflow; right: Neptune).

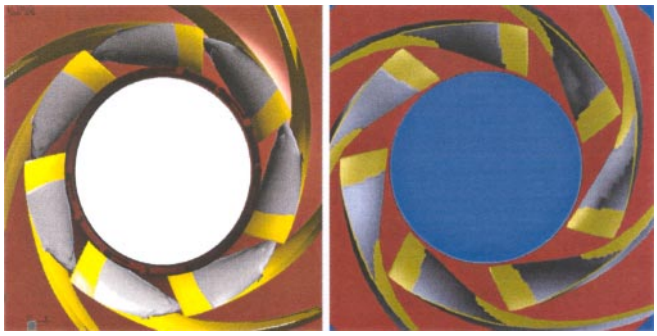

FIGURE 16
Predicted cavity for $\sigma_{u1} = 0.28$ for the improved impeller at best efficiency point ($\varphi_1 = 0.26$) (left: CFX-Tascflow; right: Neptune).

of 0.5 and 0.28, respectively; they compare well. The change in morphology of the cavities from those obtained for the original impeller is clearly visible in these figures. For this improved impeller, cavitation begins far from the vane leading, at the mid span of the blade. This cavity development results from a much more constant pressure distribution over the blade, which has been induced by the improved design.

For this impeller, the head impairment predicted by CFX-Tascflow was underestimated and, contrary to the previous impeller, started at a lower cavitation coefficient than the measured one, as shown in Figure 17. This led to an underestimated cavitation coefficient corresponding to the 3% head impairment threshold.

The prediction for the flow rates obtained with the noncoupled method (Neptune) agrees fairly well with the measured inception and 3% head drop curves. This head impairment limit is nevertheless slightly overestimated at partload and underestimated at overload. The prediction shows a local maximum in the cavitation inception curve at a flow coefficient of 0.2. This

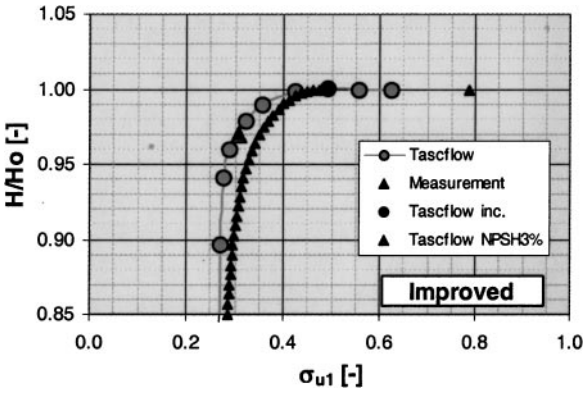

FIGURE 17
Measured and predicted (CFX-Tascflow) relative head impairment as a function of the cavitation index of the improved impeller.

local peak is not shown by the measurement but mainly because no measurement is available for this particular flow.

CONCLUSIONS

A benchmark for commercial codes was established using the calculations made by code vendors. This benchmark has shown CFX-Tascflow to be the most appropriate code for predicting cavitation performance regarding accuracy and for computing time in the process of an impeller design. This is because the method used in this code corresponds to a steady approach and is therefore much faster then the other codes that are using methods with unsteady approaches. Contrary to CFX-Tascflow, which performed a flow analysis in the impeller alone, the other code vendors chose to perform a calculation in the whole pump. This partially explains the large differences in the calculation times.

The results obtained with CFX-Tascflow for two similar nq = 33 impellers were compared with those of a simple cavity prediction method. The latter method is based on the solving of the Rayleigh-Plesset equation using the noncavitating pressure distribution along grid lines obtained using a three-dimensional Navier-Stokes equation. This simple approach has been shown to provide, in a very short time, predictions about cavity morphology as well as inception and 3% head impairment limits as accurate as those obtained with CFX-Tascflow. This simple method is, of course, far from the real physical, neglecting the influence of the cavity development on the main flow, but it is quite well suited for impeller design. The cavitation model implemented in the available commercial CFD codes are today too time expensive for this purpose and their accuracy does not yet justify such a time investment.

NOMENCLATURE

H	total head
Q	flow rate
g	acceleration due to gravity
L_c	cavity length
p	static pressure
p_v	vapor pressure of pumped liquid
n	rotational speed in rad·s^{-1}
n_q	specific speed of pump $n\frac{\sqrt{Q}}{H^{0.75}}$
NPSH	net positive suction head, $\frac{p_a - p_s}{2g} - H_s$
T_{1a}	inlet pitch at shroud
U	blade tip peripheral speed

Greek Letters

φ_1	flow coefficient $\frac{2gH}{U_1^2}$
σ_{u1}	cavitation coefficient $\frac{2g\text{NPSH}}{U_1^2}$

Subscripts

BEP	best efficiency point
inc	incipient condition
s	pump suction
1	impeller eye
2	impeller outlet

REFERENCES

Arn, C., Avellan, F., and Dupont, P. 1998, April. Prediction of Francis turbines efficiency alteration by traveling bubble cavitation, 81–86. *Proceedings of the 3rd International Symposium on Cavitation*, Grenoble, France.

Casartelli, E., Evertz, H., Gyarmathy, G., and Saxer, A. 1995. Secondary flows in a centrifugal compressor stage as predicted by steady viscous flow computations. *Proceedings of the 2nd International Conference on Heat Engines and Environmental Protection*. Balatonfuered, Hungary.

Combes, J.-F., and Archer, A. 2000, November. Etude de l'erosion de cavitation dans la pompe SHF. *Proceedings de la 164ème session du Comité Scientifique et Technique de la SHF, Machines Hydrauliques-Instationnarités et Effets Associés, Colloque d'Hydrotechnique*. Chatou, France.

Delonnay, Y. 1989. Modélisation d'Écoulements *Instationnaires et Cavitants* (thèse, Institut National Polytechnique de Grenoble, France). In French.

Delonnay, Y., and Kueny, J. 1990. Two-phase flow approach in unsteady cavitation modeling. *Proceedings of the cavitation and multiphase flow forum 98*. Toronto: ASME.

Dieval, L., Marcer, R., and Arnaud, M. 1998, April. Modélisation de poches de cavitation par une méthode de suivi d'interfaces de type VOF. *Proceedings of the 3rd International Symposium on Cavitation*. Grenoble, France.

Dupont, P. 2001, March. Numerical prediction of cavitation in pumps. *Proceedings of the 18th International Pump Users Symposium*. Houston, Texas,

Dupont, P., and Avellan, F. 1991, June. Numerical computation of a leading edge cavity. Cavitation '91 Symposium, *Proceedings of the 1st ASME-JSME Fluids Engineering Conference*. Portland, Oregon.

Favre, J.-N., Avellan, F., and Ryhming, I. L. 1987, October. Cavitation performance improvement using a 2-D inverse method of hydraulic runner design. *Proceedings of the International Conference on Inverse Design Concepts and Optimization in Engineering Science-II (ICIDES)*. Pennsylvania State University.

Goto, A. 1997, June. Prediction of diffuser pump performance using 3-D viscous stage calculation. *Proceedings of the ASME Fluids Engineering Division Summer Meeting, Paper FEDSM97-3340*. Vancouver, Canada: ASME.

Guelich, J., Favre, J.-N., and Denus, K. 1997, June. An assessment of pump impeller performance predictions by 3D-Navier-Stokes calculations. *Proceedings of the ASME Fluids Engineering Division Summer Meeting*. Vancouver, Canada: ASME.

Hirschi, R., Dupont, P., Avellan, F., Favre, J.-N., Guelich, J.-F., Handloser, W., and Parkinson, E. 1997, June. Centrifugal pump performance drop due to leading-edge cavitation: numerical prediction compared with model tests. *Proceedings of the 1997 ASME Fluids Engineering Division Summer Meeting*. Vancouver, Canada: ASME.

Hirschi, R., Dupont, P., Avellan, F., Favre, J.-N., Guelich, J.-F., Handloser, W., and Parkinson, E. 1998a. Centrifugal pump performance drop due to leading-edge cavitation: numerical predictions compared with model tests. *Journal of Fluids Engineering* 120:705–711.

Hirschi, R., Dupont, P., and Avellan, F. 1998b, April. Partial sheet cavities prediction on a twisted elliptical planform hydrofoil using a fully 3-D approach. *Proceedings of the 3rd International Symposium on Cavitation*. Grenoble, France.

Kaenel, A., Morel, P., Maitre, T., Rebattet, C., and Kueny, J.-L. 1995. 3-D partial cavitating flow in a rocket turbopump inducer: numerical predictions compared with laser velocimetry measurements. *Proceedings of the International Symposium on Cavitation*, 57. Deauville, France.

Kinnas, S. A., and Fine, N. E. 1993. A numerical nonlinear analysis of the flow around two- and three-dimensional partially cavitating hydrofoils. *Journal of Fluid Mechanics* 254:151–181.

Kubota, A., Kato, H., and Yamaguchi, H. 1989, September. Finite difference analysis of unsteady cavitation on a two-dimensional hydrofoil. *Proceedings of the 5th International Conference Numerical Ship Hydrodynamics*. Hiroshima, Japan.

Kubota, A., Kato, H., and Yamaguchi, H. 1992. A new modeling of cavitating flows: a numerical study of unsteady cavitation on a hydrofoil section. *Journal of Fluid Mechanics* 240:56–96.

Lemonnier, H., and Rowe, A. 1988. Another approach in modeling cavitation flows. *Journal of Fluid Mechanics* 195:557–580.

Maître, T., and Kueny, J. L. 1990. Three-dimensional models of cavitation in rocket engine inducers. Fluid Machinery Forum. Toronto, Canada: ASME.

Muggli, F. A., Wiss, D., Eisele, K., and Casey, M. V., 1994. Flow analysis in a pump diffuser, 2: Validation and limitations of CFD for diffusers flow. *Journal of Fluids Engineering* 119:968–977.

Reboud, J. L., Stutz, B., and Coutier, O. 1998. Two-phase flow structure of cavitation: experiment and modelling of unsteady effects. *Proceedings of the 3rd International Symposium on Cavitation*. Grenoble, France.

Soyama, H. 1995. Vibration and noises associated with severe cavitation erosion arisen in high specific speed centrifugal pump. 225–232. *Proceedings of the International Symposium on Cavitation*. Deauville, France.

Spring, H. 1992. Affordable quasi three-dimensional inverse design method for pump impellers, 97–110. *Proceedings of the 9th International Pump Users Symposium*. Houston, TX.

Tamura, Y., Sugiyama, K., and Matsumoto, Y. 2001. Physical modeling and solution algorithm for cavitating flow simulations, 2001–2652. *15th AIAA Computational Fluid Dynamics Conference*. Anaheim, CA. AIAA.

Uhlman, J. S. 1983. *The Surface Singularity Method Applied to Partially Cavitating Hydrofoils* (PhD diss, Massachusetts Institute of Technology).

Ukon, Y. 1980. Partial cavitation on two- and three-dimensional hydrofoils and marine propellers, 195–206. *Proceedings of the 10th AIRH Symposium*. Tokyo, Japan: AIRH.

Visser, F. C. 2001, May. Some user experience demonstrating the use of computational fluid dynamics for cavitation analysis and head prediction of centrifugal pumps. *Proceedings of ASME FEDSM'01*. New Orleans, Louisiana: ASME.

Zangeneh, M., Goto, A., and Takemura, T. 1996. Suppression of secondary flows in a mixed-flow pump impeller by application of three-dimensional inverse design method. 1: Design and numerical validation. *Transactions of ASME* 118:536–551.

Zangeneh, M., Goto, A., and Harada, H. 1998. On the design criteria for suppression of secondary flows in centrifugal and mixed flow impellers. *Journal of Turbomachinery* 120:723–735.